J Mol Model (2013) 19:661–672
DOI 10.1007/s00894-012-1581-2

ORIGINAL PAPER

Ion disturbance and clustering in the NaCl water solutions

Qiang Zhang · Xia Zhang · Dong-Xia Zhao

Received: 31 January 2012 / Accepted: 22 August 2012 / Published online: 23 September 2012

Abstract Ion clustering and the solvation properties in the NaCl solutions are explored by molecular dynamics simulations with several popular force fields. The existence of ions has a negligible disturbance to the hydrogen bond structures and rotational mobility of water beyond the first ion solvation shells, which is suggested by the local hydrogen bond structures and the rotation times of water. The potential of mean force (PMF) of ion pair in the dilute solution presents a consistent view with the populations of ion clusters in the electrolyte solutions. The aggregation level of ions is sensitive to the force field used in the simulations. The ion-ion interaction potential plays an important role in the forming of the contact ion pair. The entropy of water increases as the ion pair approaches each other and the association of ion pair is driven by the increment of water entropy according to the results from the selected force fields. The kinetic transition from the single solvent separated state to the contact ion pair is controlled by the enthalpy loss of solution.

Keywords Force field · Ion pairing · Ion solvation · Potential of mean force · Molecular dynamics simulations

Introduction

Ion solvation and ion clustering in water solutions is a fundamental topic of physical chemistry [1, 2]. The ion induced effect on the water hydrogen bond (H-bond) structures has been explored extensively, but there is still no solid conclusion. Now, the debate focuses on the range of the ion induction to the water H-bond structures. The results from the 2D-IR experiments suggest that no remarkable perturbation has been found beyond the first ion solvation shell for the monovalent ions from the angle of water rotation [3–5]. However, the computer simulations present a controversial picture that the perturbation effect can extend to the third solvation shell from the angle of the solvation energy and the H-bond coordination number of the single water around the ion [6, 7] and results in the shell shifting inward for the water-water radial distribution function [8]. The previous study revealed that the effect of ions and counterions on water can be strongly interdependent and nonadditive [5]. The further explorations in the molecular level are needed to make sure whether the two directions point to the same origin.

Ion pairing in the electrolyte solutions is also an attractive theme in the chemical and biological fields. Study on the ion association in water solutions has been reviewed by Marcus [1] and Collins [9]. Ion pairing is well-documented for aqueous solutions of 1:1 strong electrolytes by the experiments, as well as molecular dynamics simulations [10–14]. The water affinity of ions and the thermodynamics of ion clustering have been explored, as well as the ion pairing effect on the solvent structure and H-bond dynamics [12, 14]. In general, the ions with the opposite charges can associate together and the possibility of ion clustering is closely related to the factors, such as the ion size, sign and magnitude of ion charge, concentration etc. The characteristic solvation structures of the ion pair are usually classified into three types in the water solutions: double solvent separated ion-pair (2SIP), single solvent separated ion-pair (SSIP), and contact ion pair (CIP) respectively [1]. However, there are still no sufficient reports about the ion pairing effect on the solvation properties in the electrolyte solutions at

Q. Zhang (✉) · X. Zhang
Institute of Chemistry, Chemical engineering and food safety,
Bohai University,
Jinzhou 121000, China
e-mail: zhangqiang@bhu.edu.cn

D.-X. Zhao
Institute of Chemistry and Chemical engineering,
Liaoning Normal University,
Dalian 116029, China

molecule level. Additionally, the previous studies show that the association level and rate of ions strictly depends on the potential models used in the simulations [12–14]. The artificial results and the overestimation of the ion clustering in the simulations have been observed in the simulations [15, 16], which is ascribed to the mismatch of ion-ion and ion-water interaction potential. Great care should be taken in choosing balanced ionic parameters even when using the most popular force-fields [16].

In this work, a series of simulations were carried out to explore the ion solvation structures, ion effect on the hydrogen bond network of water and ion aggregation in NaCl aqueous solutions at different concentrations. The thermodynamic enthalpy and entropy in the process of ion pairing are derived from the potential of mean force (PMF) with the popular force fields [10, 17–23]. The thermodynamic origin of ion pairing and the force field dependent issue will be discussed in this paper.

Simulation methods and simulation details

Simulation potentials and detail

The previous studies suggested that the ion association is closely related to the model used in the simulations [14–16]. For the sake of argument and comparison, five LJ 12-6 models (Dang [10], CHARMM [20], AMBER [21], OPLS [22], GROMOS [23]) and BMHTF [17–19]) for ion-ion interactions are considered here. The Dang Cl^- parameters are used for the AMBER force field. The SPC/E [24], TIP3P [25] and SPC [26] water models are used for the NaCl water solutions in a consistent way in Table 1. The Dang ion-water potential was used for the BMHTF model [10, 27]. The average polarization effect is considered in the SPC/E model. Dang ion model was designed for the RPOL and SPC/E water model and parameterized by fitting the experimental data, so it should be consistent with the SPC/E model. The studies by Sanz, Horinek and their coworkers suggest that the Dang ion-water interaction potential can reasonably reproduce the experimental ion solvation properties [28]. The BMHTF ion model initially was optimized for the molten salt. It can reproduce the melting point of NaCl reasonably [17–19, 28] and the acceptable activity coefficients of NaCl in the water solutions with the Dang ion-water potential [27]. For the water-water and water-ion interactions, as well as the ion-ion interactions for LJ 12-6 model, the potential function is given as:

$$u_{ij} = 4\varepsilon_{ij}\left[\left(\frac{\sigma_{ij}}{r_{ij}}\right)^{12} - \left(\frac{\sigma_{ij}}{r_{ij}}\right)^{6}\right] + \frac{q_i q_j}{4\pi\varepsilon_0 r_{ij}} \quad (1)$$

Where i and j index the oxygen atom of water or ions, q_i is the charge parameter of the atom in water or ion. σ_{ij} and ε_{ij} are derived by the Lorentz-Berthelot rules $\sigma_{ij}=(\sigma_{ii}+\sigma_{jj})/2$

Table 1 Force field parameters and ion solvation energies

Atom	ε (kcal/mol)	σ (Å)	q (e)	ΔG_{solv} (kcal/mol)[42]	ΔS_{solv} (kcal/mol)[42]
O water (SPC/E)	0.1554	3.166	−0.8476		
H water (SPC/E)	0.000	0.000	0.4238		
O water (SPC)	0.1554	3.166	−0.82		
H water (SPC)	0.000	0.000	0.41		
O water (TIP3P)	0.1521	3.151	−0.834		
H water (TIP3P)	0.000	0.000	0.417		
Na^+ (Dang)	0.13	2.35	+1.0	−97	−4
Cl^- (Dang)	0.1	4.4	−1.0	−73	−47
Na^+ (OPLS)	0.0005	4.07	+1.0	−89	−0.2
Cl^- (OPLS)	0.71	4.02	−1.0	−76	−49
Na^+ (AMBER)	0.003	3.33	+1.0	−95	−2
Cl^- (AMBER)[a]	0.1	4.4	−1.0	−73	−47
Na^+ (CHARMM)	0.05	2.43	+1.0	−98	−4
Cl^- (CHARMM)	0.15	4.05	−1.0	−75	−49
Na^+ (GROMOS)	0.015	2.58	+1.0		
Cl^- (GROMOS)	0.11	4.45	−1.0		
Ion pair (BMHTF)	A_{ij} (kcal/mol)	ρ_{ij} (Å)	C_{ij} (kcal Å^6/mol)	D_{ij} (kcal Å^8/mol)	
Na^+-Na^+	9768	0.317	24	11	
Na^+-Cl^-	28938	0.317	161	200	
Cl^-- Cl^-	80368	0.317	1670	3354	

[a]The parameters of Cl^- in AMBER force field come from Dang model directly

(CHARMM-TIP3P, BMHTF-SPC/E and Dang-SPC/E potentials) or geometric rule $\sigma_{ij}=(\sigma_{ii}\sigma_{jj})^{1/2}$ (AMBER-TIP3P, OPLS-TIP3P and GROMOS-SPC) and $\varepsilon_{ij}=(\varepsilon_{ii}\ \varepsilon_{jj})^{1/2}$. The relevant parameters and the combined potentials were listed in Table 1. For the ion-ion interactions with BMHTF potential has the following form:

$$u_{ij}(r) = q_i q_j / r + A_{ij} \exp\left(-r_{ij} \Big/ \rho_{ij}\right) - C_{ij}/r^6 - D_{ij}/r^8 \qquad (2)$$

Where the first term is the Coulombic interaction, the second Born-Huggins exponential repulsion with parameters obtained by Tosi and Fumi, and the third and fourth terms are, respectively, the dipole-dipole and dipole-quadruple dispersion energies with parameters obtained by Mayer [17–19, 27]. The potential parameters are also summarized in the Table 1.

The NaCl water solutions at the concentrations of 0.3 $molL^{-1}$, 1 $molL^{-1}$ and 2 $molL^{-1}$, as well as a series of water bulks with just one pair of NaCl fixed at the different distances, were set up. The number of water in each simulation bulk was kept at 500 and NaCl was added into the simulation box according to the concentration of each solution. For the starting configuration, the molecules are located at random positions and orientations and the ions randomly distributed in the cubic volume. Initial velocities are generated assuming a Maxwell-Boltzmann distribution, and they are rescaled to guarantee momentum conservation. A 500 ps NPT pre-equilibrated simulation for each solution is performed at 350 K and 1 atm to obtain the reasonable configuration, then the quenching simulations were carried out from 350 K to 300 K with the annealing rate of 50 psK^{-1} to reach the equilibration. MD runs of 2 ns were used to equilibrate each system at 290 K, 300 K and 310 K respectively. At last, the equilibration simulations are run for another 5 ns to calculate properties of solutions. The self-diffusion constant of Na^+ ion (the slowest component in the solutions) is in the range of 0.6~1.5 $10^{-5}cm^2/s$ at the concentration of 2 $moll^{-1}$ (0.9~2.0 $10^{-5}cm^2/s$ at 1 $moll^{-1}$) for the different potentials, so the ions and water can diffuse across the cubic cell (about 25 Å for the cell length) within the equilibration time. The previous work suggests that the NaCl solution of 1 $moll^{-1}$ can reach equilibration within a time scale of approximately 1 ns [12]. The weak coupling scheme according to Berendsen et al. [29] were used with the coupling time constant of 1 ps. The periodic boundary conditions and minimum image convention are adopted. The non-bonded van der Waals interactions are truncated at 10 Å with switching function and the particle mesh Ewald summation technique [30] is used to treat the long-range Coulomb interaction. The simulation trajectories are saved every 100 fs. All simulations are performed with the Tinker simulation code [31].

Potential of mean force

The PMFs are usually utilized to identify the thermodynamic states and study the kinetic process of ion pairing (CIP, SSIP and 2SIP) [10, 14–16, 32]. The constraint molecular dynamics were run to obtain the PMFs of the Na^+-Cl^- ion pair within the range of 1.8~12 Å in pure water [10, 14]. The SHAKE algorithm was used to fix the distances of Na^+-Cl^-. The integration step of PMF is 0.2 Å. A 2 ns simulation was run at each distance r to obtain the mean force.

The mean force between the ion pairs has been determined by the sum of the mean force exerted by the water molecules, $\Delta F(r)$, and the direct force $F_d(r)$ between the ions.

$$F(r) = F_d(r) + \Delta F(r) \qquad (3)$$

In the above equation, $\Delta F(r)$ is the mean force exerted by the water molecules on the ion pair. This can be expressed as

$$\Delta F(r) = \left\langle \vec{r}_p \cdot \left(\vec{F}_{AS} - \vec{F}_{BS}\right)\right\rangle / 2 \qquad (4)$$

Where F_{AS} and F_{BS} are the forces due to the water interactions on the Na^+ and Cl^-, respectively, and r_p is a unit vector along the ion pair Na^+-Cl direction. The mean force potential relative to the potential energy $W(r_0)$ at r_0, $W(r)$, was obtained by the integration of the total force [14].

$$W(r) = W(r_0) - \int_{r_0}^{r} F(r)dr \qquad (5)$$

The upper limit r_0 of the integration was taken to be 12 Å. The macroscopic Coulomb potential at r_0, $W(r_0)=q_iq_j/\varepsilon r$, is used as the original value as in previous work [10, 14]. The q_i and q_j are the ionic charges and ε is the dielectric constant of pure water at 298 K and 1 atm. The experimental dielectric constant of water, ε=78, has been taken for any case. Because the ion-ion distance was fixed in the constrained simulations, which reduces the ion entropy in the phase space, the resulting volume-entropy force, $-2k_BT/r$, needs to be taken into account in Eq. 3. Now, the total PMF of Eq. 5 can be revised as [32, 33]:

$$W(r) = -\int_{r_0}^{r} \bar{F}(r')dr' + 2k_BT \ln r + W(r_0). \qquad (6)$$

Definitions of hydrogen bond and subspecies of water

Hydrogen bond Two water molecules are considered to be hydrogen-bonded when the distance between their oxygen atoms and the angle between the vector joining the two oxygen atoms and the OH bond of the H-bond donating water molecule, is not bigger than 3.5 Å and 30°.

Subspecies definition of water Water molecules can be simply classified into three subspecies according to its surrounding environments. (1) bulk water: there are only water molecules in the first solvation shell (no more than 3.5 Å); (2) Na^+ shell water (no more than 3.2 Å): only Na^+ in the first solvation shell of water, no Cl^-; (2) Cl^- shell water (no more than 4.0 Å): only Cl^- in the first solvation shell of water, no Na^+. The water in both shells of Na^+ and Cl^- is not considered here for simple consideration.

Results and discussion

We mainly focus on two open questions: one is the ion effect on the water structures and dynamics in the NaCl water solutions. The other is the ion clustering and the thermodynamic nature of ion pairing. The force field dependent issue will also be discussed in this part.

The local structures and ion perturbation

The structures of the NaCl solutions extracted from the simulations with the Dang- SPC/E model are presented here. The coordinate water numbers of Na^+ and Cl^- within their first solvation shells are about 6.0 and 6.6 respectively and weakly dependent on the concentration, the corresponding value from 5 to 8 suggested by the experiments and simulations [34, 35]. The solvation shell of Na^+ is more compact than that of Cl^-. The average distances for the pair of Cl^--Ow and Na^+-Ow are 3.32 and 2.46 Å for any concentration, corresponding to the first peaks of $g_{Cl\text{-}Ow}(r)$ and $g_{Cl\text{-}Ow}(r)$ in the lowest panel of Fig. 3c and d.

The influence of ion on the H-bond structures of water and the structures of the ion hydration shells is highly specific to the individual ion [3–5, 8]. One divergence between distinct experimental and theoretical results on ionic hydration is that the perturbations of the H-bond network of water from ions are restricted to their first hydration shells or not. In current solutions, the average H-bond numbers of water are 3.61, 3.50, 3.32 and 3.06 in pure water, 0.3 $molL^{-1}$, 1 $molL^{-1}$ and 2 $molL^{-1}$ solutions. However, the H-bond number for bulk water in any solution is 3.59, nearly no change with concentration. In Fig. 1, the first and second peak can be found clearly in the pair radial distribution functions of $g_{OwOw}(r)$ for the pure and dilute solutions. The second and third shell peaks shifts inward with increasing the ion concentration. The boundary between them has been obscured at 2 $moll^{-1}$. A similar phenomenon is also found in the previous studies [6–8]. There is a negligible difference for the $g_{OwOw}(r)$ within the current range of concentrations for the BMHTF-SPC/E and Dang-SPC/E models. Two overlap curves from two potentials at 2 $molL^{-1}$ are shown in the Fig. 1 (middle).

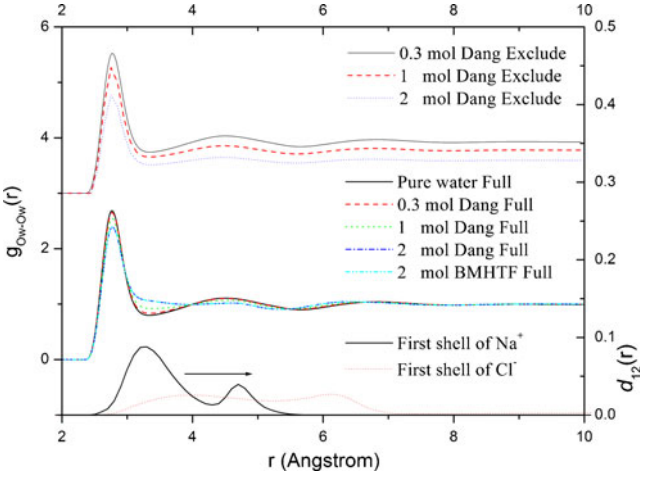

Fig. 1 The pair radial distribution function $g_{OwOw}(r)$ of the NaCl solutions and pure water (*middle*), and the $g_{OwOw}(r)$ excluding the water in the first ion solvation shells (*top*), the distribution functions $d_{12}(r)$ in the ion first solvation shells (*below*)

The spatial distribution functions at the concentrations of 0.3 $molL^{-1}$ and 2 $molL^{-1}$ are shown in Fig. 2. The first and second shell of water can evidently be found there. There are no evident changes for the shape, spatial position and extension level in the solutions at the different concentrations.

The structural information in the solutions has been analyzed by the radial and spatial distribution functions averagely. Now, the local H-bond structures of water are presented here. Firstly, let's focus on the H-bond structures of water with the separation r between the ion and water or water and water. The radial distribution functions, $N_{HB}(r)$, $\theta(r)$ and $R_{Ow\text{-}Ow}(r)$, are shown and defined in Fig. 3. The H-bond number of water in Fig. 3a and b, $N_{HB}(r)$ is closely correlated with the distance r. The local information is lost beyond the first two H-bond shells (6 Å). When the H-bond water pair at closest region, larger H-bond number, $N_{HB}(r)$, and smaller the H-bond angle and distance, $\theta(r)$ and $R_{Ow\text{-}Ow}(r)$, are found in Fig. 3a. The tendency of $N_{HB}(r)$ with r appears consistent with that of $g_{OwOw}(r)$. There are larger values of $N_{HB}(r)$ around the first and second peaks of $g_{OwOw}(r)$ than that at median range between them. The decrement of water H-bond number and the increments of $\theta(r)$ and $R_{Ow\text{-}Ow}(r)$ within this interval are due to the H-bond exchange of water from the first H-bond shell to the second shell [36]. The donating and accepting H-bond structures of water are similar to each other. The similar case is also found for the bulk water of NaCl solution in Fig. 3b.

There is a strong disturbance to the structures of the accepting H-bond for the water in the first solvation shell of the Na^+ and a negligible effect on the donating H-bond, which can be seen from $N_{HB}(r)$ within this range in Fig. 3c. A large $R_{Ow\text{-}Ow}(r)$ and $\theta(r)$ at smaller r (<3.2 Å) results from the electrostrictive effect of Na^+ on water oxygen atom, which prevent water from forming the water-water

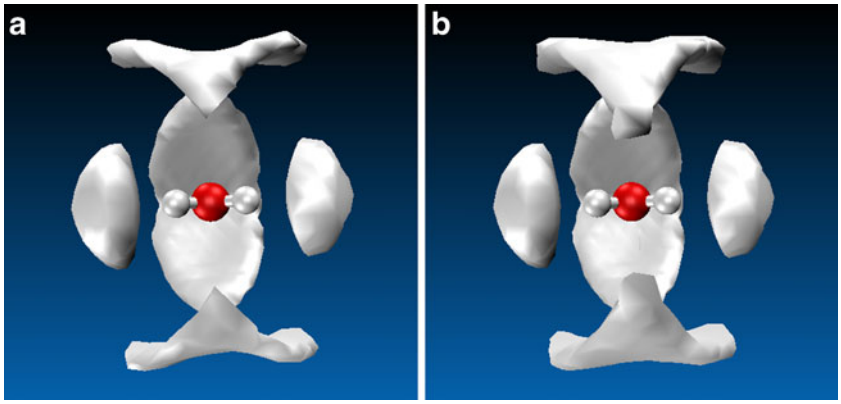

Fig. 2 The spatial distributions of water around the central water in the 0.3 $moll^{-1}$ (**a**) and 2 $moll^{-1}$ (**b**) solutions. The isovalue contour of water oxygen density around the central water from Dang-SPC/E model, the local coordination defined with the central water

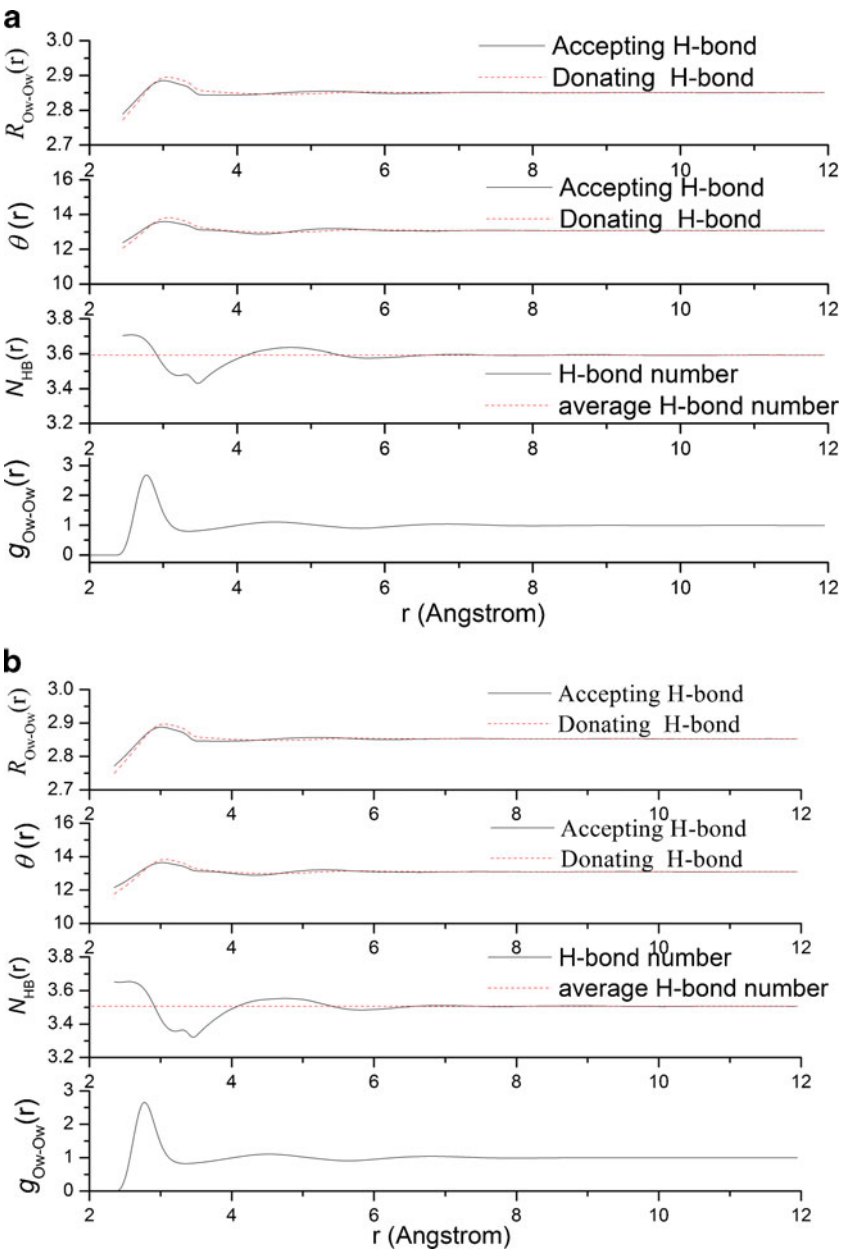

Fig. 3 The radial distribution functions, $N_{HB}(r)$, $\theta(r)$ and $R_{Ow\text{-}Ow}(r)$ is the average H-bond number, the H-bond angle and the H-bond length of the water with the separation r to the ion or water oxygen. **a** water oxygen origin in pure water; **b** bulk water oxygen origin; **c** Na^+ origin; **d** Cl^- origin

Fig. 3 (continued)

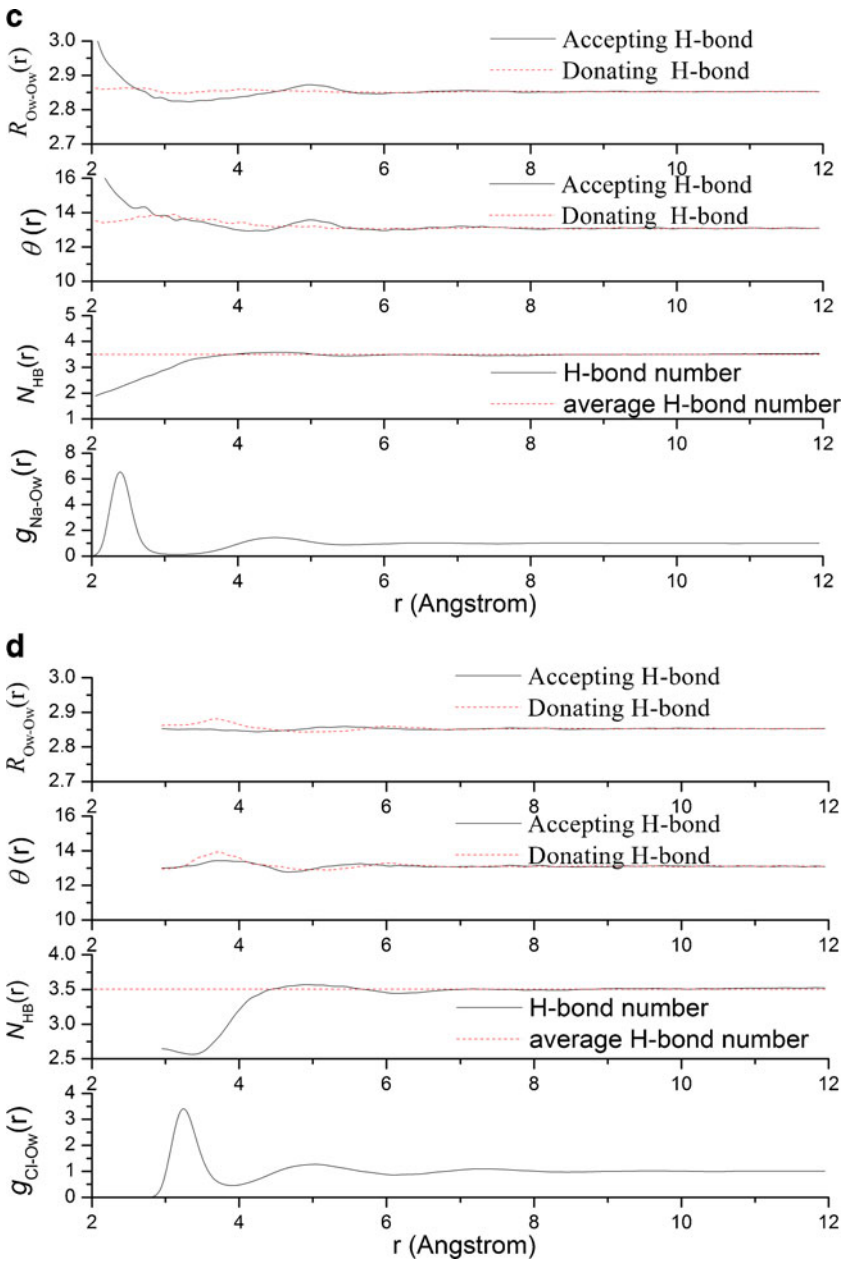

accepting H-bond. With the elongation of Na^+-water pair, the accepting H-bond can be formed and the H-bond bond number, angle and length approach their average values respectively. Then the water has moved from the first solvation shell to the second shell of Na^+ at about 4.5 Å. There is a weak distortion of the accepting H-bond of water at the distance of 4.8 Å compared with the values for water origin. However, the effect of Cl^- is very small at whole range of r and a small disruption to the H-bond structure of water in its first solvation shell, which can be found for $R_{Ow\text{-}Ow}(r)$ and $\theta(r)$ in Fig. 3d. The size of the chloride shell is similar to the water, which indicates chloride is not a strong "breaker" for the water hydrogen bond structures relative to sodium [37].

The previous publications suggest that the ion perturbation can extend outside the first hydration shell of water and the shifting inward of the second and third peaks of $g_{OwOw}(r)$ results from the induction effect under the electric field of ion like the pressure effect on water structures [6–8]. We also calculated the average H-bond distance R_{12} and the neighbor H-bond angle θ in the water tetrahedral structure unit (R_{12} and θ defined in Fig. 4a), which can be used to locate the positions of first and second peaks of $g_{OwOw}(r)$ and exclude the contribution from the water pair in the first solvation shells of ions [8]. The value of R_{12} is about 2.85 Å at any concentration and the angles θ are 107.7°, 107.3° and 106.8° in the 2 $moll^{-1}$, 1 $moll^{-1}$ and 0.3 $moll^{-1}$ solutions respectively. Then, the R_{13} value can be derived according to the R_{12} and θ. Its value is

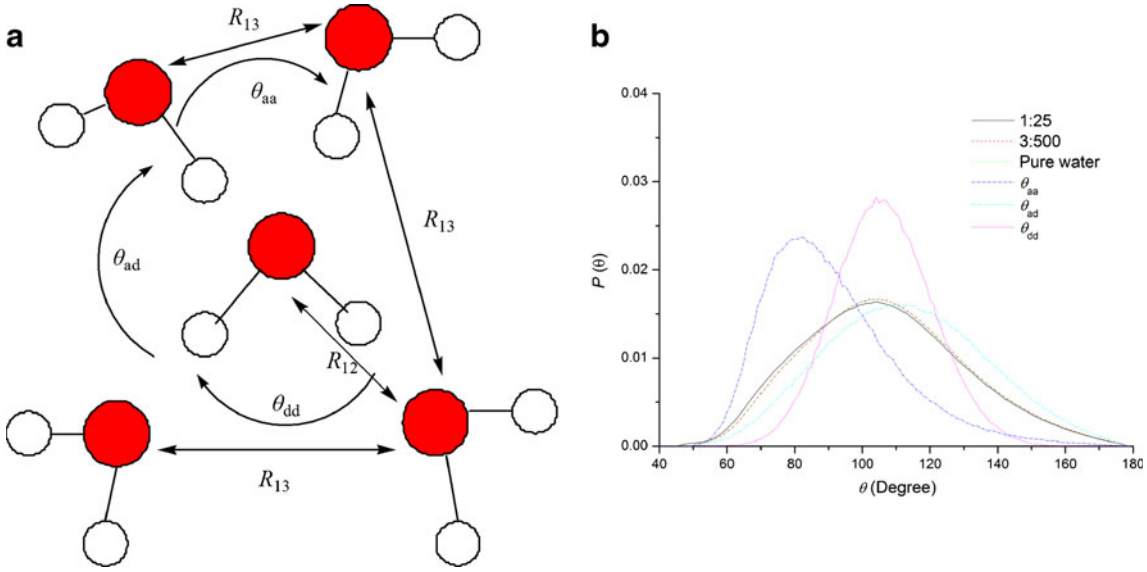

Fig. 4 **a** The tetrahedral H-bond structure of water, R_{12}: the distance of two oxygen atoms of any two water molecules H-bonding to each other; R_{13}: the distance between two oxygen atoms of two water molecules both H-bonding to the central water molecule; θ_{aa}: the angle between two neighbor accepting H-bond pair Ow-Ow vectors; θ_{ad}: the angle between one accepting H-bond Ow-Ow vector; θ_{dd}: the angle of two neighbor donating H-bond Ow-Ow vectors; **b** the distribution of θ in the 2 moll^{-1}, 0.3 moll^{-1} and pure water solutions, as well as three components θ_{aa}, θ_{ad} and θ_{dd} for he pure water

almost kept at about 4.50 Å for any concentration, which suggests that the position of the second peak of $g_{OwOw}(r)$ does not shift with adding NaCl into the water, if excluding the contribution of water in the ion solvation shells. We also analyzed the distance distribution function $d_{12}(r)$ between any pair of waters in the ion first solvation shells in Fig. 1 (below). One interesting fact is found by comparing it to the full functions of $g_{OwOw}(r)$ in Fig. 1 (middle). The shoulder at 3.5 Å should stem from the contribution of water-water radial distribution in the first Na^+ solvation shell. The second peak shifting of the $g_{OwOw}(r)$ mainly results from the Na^+ solvation structure and the third peak shifting from the Cl^- solvation structure. The existence of Na^+ and Cl^- does not substantially alter the H-bond structure of water beyond the first solvation shells. On the other hand, the distribution curve of the neighbor H-bond angle is shown in Fig. 4b. The donor-donor angle θ_{dd} fluctuates around the average value. The sodium ion occupies the acceptor H-bond sites of water oxygen and only two donor H-bonds exist, so that the sodium ion should not affect the average value of the neighbor H-bond angle. For the existence of the chloride ion, the cancel effect can be found between θ_{ad} and θ_{dd}, because of the probabilities of the acceptor-donor and donor-donor structures in the first Cl^- shell at same level. The total distribution functions of θ at 2 moll^{-1}, 0.3 moll^{-1} and in pure water are very similar. The $g_{OwOw}(r)$ excluding the water within the first solvation shells are shown in Fig. 1 (top). The shifting of the second and third peaks relative to pure water becomes very small, which is consistent with the results obtained from the analysis of the neighboring H-bond length and H-bond angle, as well as the radial distribution functions of H-bond properties above. So, one conclusion can be made that the broadening and shifting of the second and third peak of the $g_{OwOw}(r)$ mainly result from the contributions from the water in the ion solvation shells [8]. At the same time, the heights of shell peaks decrease with concentration due to that the ions disrupt the extension of the water H-bond network. The H-bond number of water deceases with the concentration, because the ions occupy the H-bond sites of water.

The results from the ultrafast 2D-IR spectrums [3–5] show that the ion perturbation on the water structure is just restrained within the first ion solvation shell and the reorientation relaxation time of water beyond the first ion coordination shells along the O-H bond direction is similar to the value in pure water. Here, the second order reorientation correlation functions are calculated and displayed in Fig. 5. The reorientation correlation function $C_l(t)$, is defined as a Legendre polynomial, $C_l(t) = \langle P_l[\mathbf{e}(t)\mathbf{e}(0)]\rangle$, where **e** is a unit vector, O-H or water dipole direction here. The average reorientation relaxation times do not change evidently with concentration (Fig. 5a) and are at the time scale of 2 ps, which agrees well with the experimental value 2.5 ps [3]. The initial decay of the rotation correlation is due to a fast libration process and the anisotropic rotations are observed for the long-time decay due to the difference of local environment for the water. Water molecules in the solutions can be classified into three types as the water molecule in the cation shell, in the anion shell and the bulk water defined in the previous part. The corresponding reorientation correlation functions for them are shown in Fig. 5b. The slowest

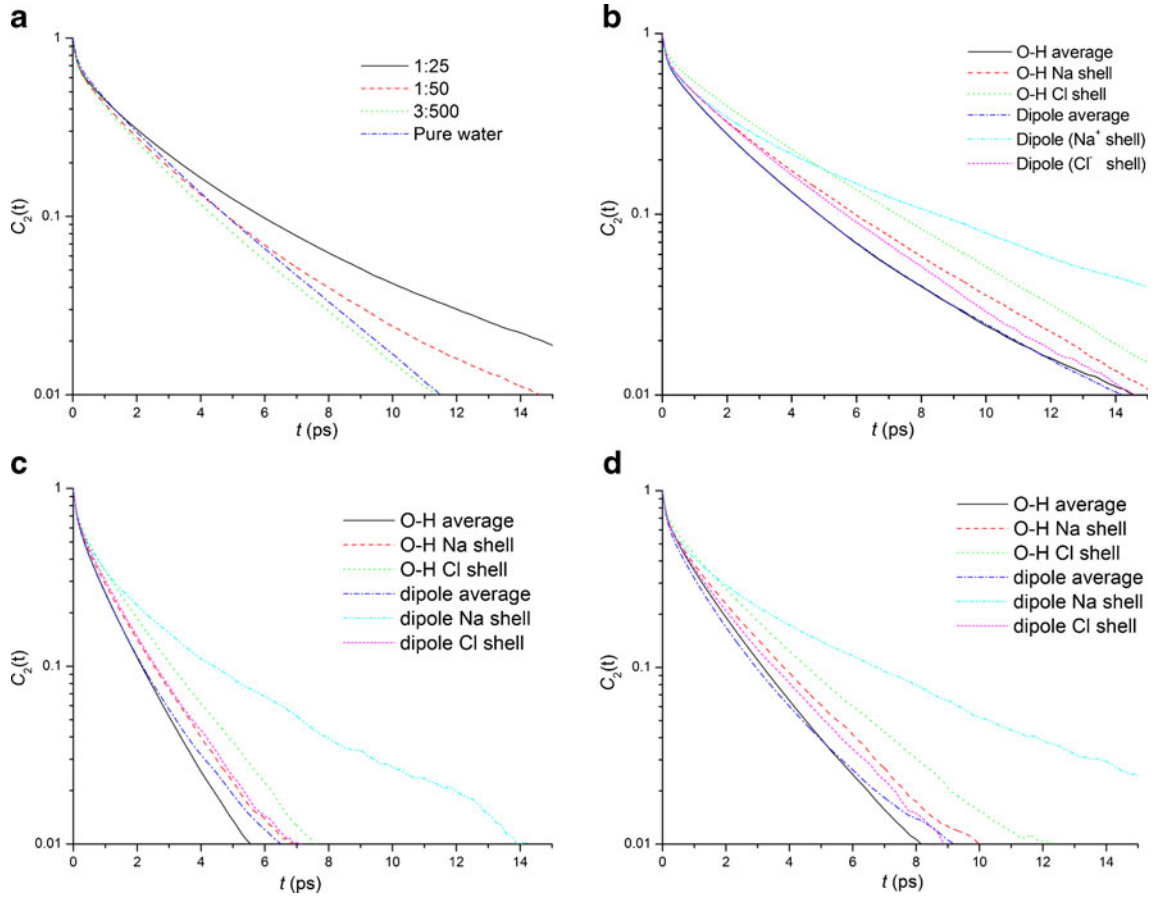

Fig. 5 **a** The reorientation correlation functions along O-H bond vector in pure water, 0.3 $moll^{-1}$, 1 $moll^{-1}$ and 2 $moll^{-1}$ NaCl solutions; $C_2(t)$ of water around the O-H bond and dipole vector in the sodium and chloride shell in the 1 $moll^{-1}$ solution with SPC/E-Dang model (**b**), AMBER-TIP3P model (**c**) and GROMOS-SPC model (**d**). The results were analyzed from the first 2 ns trajectory of 5 ns equilibration simulation. A logarithmic unit, $Log_{10}(C(t))$, is used for y-axis

component is the one in the chloride ion shell due to the stronger H-bond between water and it than the water-water H-bond. The Na^+-Ow coordinate structure does not hinder the rotation of water around the O-H bond, so the rotation of water in the first Na^+ shell is faster than that in the first Cl^- shell [28]. However, the contrary trend can be observed for the rotation around the dipole vector of water. The water dipole direction is locked by the Na^+ with the coordinate bond [5, 38]. Similar trends are shown for the rotation of water at the different environments with AMBER-TIP3P and GROMOS-SPC models as Dang-SPC/E model. Faster decays are found for them than the case for Dang-SPC/E model, due to the difference of water model. The previous publications show that the TIP3P and SPC models present higher mobility than SPC/E model [39]. The facts above indicate that the ions do not evidently affect the rotational mobility along the OH vector with the additional NaCl. The H-bond number of bulk water in any solutions is always 3.6. If there is a close relationship between the water mobility and the local structures of water, we can come to a conclusion that the ionic disturbance on the water structures is small and the ion induction on the water rotation is a local effect. The previous publications by Laage indicate that the rotational diffusion of water is controlled by the rate of the H-bond exchange reactions [36]. Further exploration should be made to uncover the mechanism of water rotation and the relationship with the local structure of water.

Ion clustering

Ion pairing and clustering in the water solutions play an important role in the protein folding, molecule recognition and some chemical reactions in the electrolyte solutions. The ion clustering level in the solutions could not be accurately determined by the experiments and is strongly dependent on the force fields used in the theoretical simulations [15, 16]. The potential of mean forces of the Na^+-Cl^- ion pair in the pure water have been calculated with the different potentials at 300 K and 1 atm. Three characteristic states of the Na^+– Cl^- ion pair are presented evidently in Fig. 6a. Among them, the CIP state is the lowest energy state, which is suggested by most of force fields

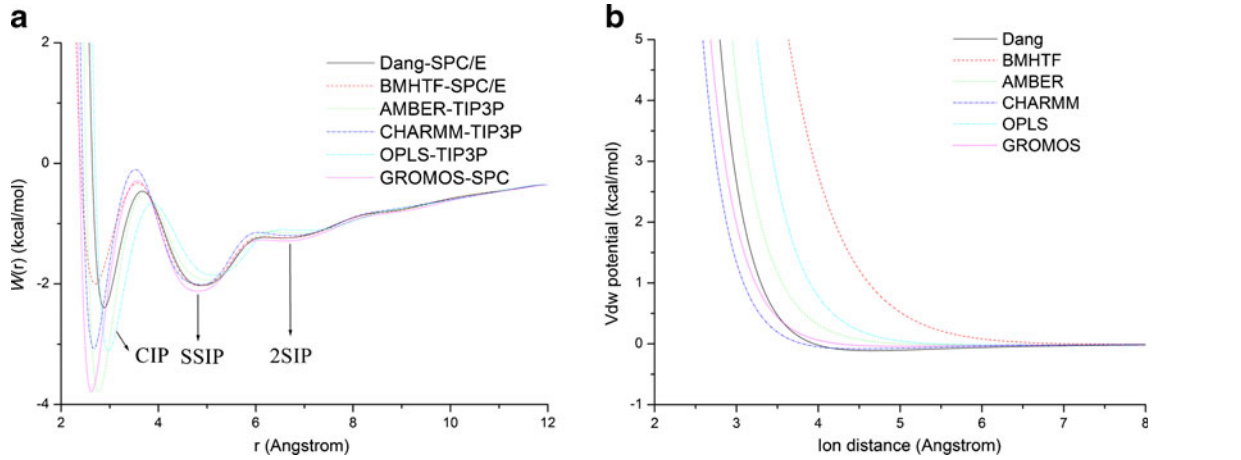

Fig. 6 **a** The potential of mean forces of the Na^+-Cl^- ion pair in the water bulks with the Dang-SPC/E, BMHTF-SPC/E, AMBER-TIP3P, CHARMM-TIP3P, OPLS-TIP3P and GROMOS-SPC force fields. **b** van der Waals potential curves of the Na^+-Cl^- pair in gas phase with the force fields as (**a**)

except the BMHTF-SPC/E model due to stronger repulsive van der Waals interaction than other potentials (Fig. 6b). The oscillation period and amplitude of the PMF curves are closely related to the sizes of ions and the specific feature of water molecule [14]. In order to evaluate the level of ion pairing quantitatively, the association constant of ion pair in the dilute solution, K_A, is defined as [1, 40]:

$$K_A \cong \frac{[NaCl]}{[Na^+][Cl^-]} = 4\pi N_A 10^{-27} \int_0^{r_C} \exp[-(W(r)/k_B T)] r^2 dr \quad (6)$$

[NaCl], [Na^+] and [Cl^-] are the ion pair, free sodium and chloride ion concentrations in dilute solution. $N_A 10^{-27}$ is a factor to convert the unit of $Å^3 \cdot molecule^{-1}$ to $L \cdot mol^{-1}$. The association constants from the simulations by the Dang-SPC/E, BMHTF-SPC/E, AMBER-TIP3P, CHARMM-TIP3P, OPLS-TIP3P and GROMOS-SPC force fields are 1.43, 0.83, 12.26, 3.21, 5.03 and 9.70 $L \cdot mol^{-1}$. The quantitative criteria for K_A cannot be given by the experimental methods [1] and theoretically depends on the model used to construct the PMF in the dilute solution [10, 12–14]. However, the relative values show that the ion pairing is very sensitive to the force fields used in the simulations. The strongest tendency of forming ion pairing can be found for the AMBER-TIP3P model according to the relative association constants. This fact is consistent with the previous prediction that the AMBER-TIP3P model overestimates the possibility of ion clustering [16]. The Dang-SPC/E and BMHTF-SPC/E potentials present a relatively lower possibility of ion pairing.

The existence of ion clusters can be anticipated in the NaCl solutions according to the association constants derived from the PMF. The NaCl solutions at 0.3, 1.0 and 2.0 $moll^{-1}$ were employed to explore the ion cluster distribution with the selected force fields described in the previous section. An ion cluster was defined as the rules [41]: (i) every ion is connected to at least one ion of the opposite charge; two ions are said to be connected if they are separated by a distance smaller than 3.5 Å; (ii) every ion can be reached from any other ion within the cluster through a path of consecutive connections. The cluster distributions in Table 2 show that the possibility and size of ion clustering increase with the concentration. The possibility of ions at non-cluster state is dominant in the solutions at any concentrations here, which is reasonable from the theoretical angle in the NaCl solutions. The Na^+ and Cl^- ions approach their

Table 2 The populations of ion cluster at 300 K from the selected force fields

Cluster size	1	2	3	4
1:25 (Dang-SPC/E)	90.9	7.6	1.2	0.2
1:25 (BMHTF- SPC/E)	96.9	2.8	0.2	
1:25 (AMBER-TIP3P)	59.0	20.2	6.8	4.7
1:25 (CHARMM-TIP3P)	83.1	12.0	3.7	0.9
1:25 (OPLS-TIP3P)	74.3	15.7	4.2	2.3
1:25 (GROMOS-SPC)	64.5	15.6	9.2	3.8
1:50 (Dang-SPC/E)	95.8	3.9	0.3	
1:50 (BMHTF-SPC/E)	98.2	1.7	0.1	
1:50 (AMBER-TIP3P)	75.2	16.4	4.9	1.9
1:50 (CHARMM-TIP3P)	90.4	6.0	2.0	0.3
1:50 (OPLS-TIP3P)	85.8	11.8	1.9	0.4
1:50 (GROMOS-SPC)	77.5	15.4	3.9	2.1
3:500 (Dang-SPC/E)	97.6	2.4		
3:500 (BMHTF-SPC/E)	99.7	0.3		
3:500 (AMBER-TIP3P)	83.2	15.1	1.6	0.1
3:500 (CHARMM-TIP3P)	96.9	3.1		
3:500 (OPLS-TIP3P)	95.7	4.3	0.1	
3:500 (GROMOS-SPC)	89.6	10.4		

theoretical solvation saturation at about 4 $moll^{-1}$ according to the coordinate numbers of the Na^+ and Cl^- ions (6.0 and 6.6 respectively). However, we also find that there is a big difference for the clustering ratio with the different potentials, over 20 % for the AMBER-TIP3P and GROMOS-SPC force fields and over 10 % for the CHARMM-TIP3P and OPLS-TIP3P force fields comparing to the values from Dang-SPC/E and BMHTF-SPC/E models at 1 $moll^{-1}$. The ratios of the cluster ion from the different potentials are qualitatively consistent with the association constants K_A at any concentration, which suggests that the free energy view of the ion pair in the dilute solution can make a constructive prediction about the ion clustering distributions. The ion-ion interaction potential plays an important role in the ion association in water solutions. More repulsive BMHTF ion-ion potential presents a little lower ion association than the LJ type Dang potential at any concentration, given the same ion-water and water-water potentials used for them. The reason may be due to the facts that the potential function forms and the calibration target properties are different in designing the force fields. The quantitative differences from the current potentials indicate that the ion clustering is also affected by the ion-water and water-water potential.

The thermodynamic origin of ion paring can be explored by dividing PMF into entropy and enthalpy subcomponents at the available distance r of ion pair, $W(r)=\Delta H(r) - T\Delta S(r)$. The entropy and enthalpy differences of system at distance r relative to infinite distance, can be derived from the following relationship:

$$\Delta S(r) = -(\partial W(r)/\partial T) = -[W_{T+\Delta T}(r) - W_T(r)]/\Delta T \quad (7)$$

$$\Delta H(r) = (\partial(W(r)/T)/\partial(1/T)) = W(r) + T\Delta S(r) \quad (8)$$

The PMFs, $W(r)$, at 290 K, 300 K and 310 K have been obtained from the constrained molecular dynamics simulations. The numerical derivatives of $W(r)$ to T can be evaluated to get the quantities above. The graphic view of the $W(r)$, $T\Delta S$ and ΔH at distance range of 1.8 ~ 12 Å from the six force fields are shown in the Fig. 7. The contribution from the relative entropy change of the constrained ion pair to the limiting distance of 12 Å, $T\Delta S_{IP}=2k_BT(\ln(12) - \ln(r))$, is also presented in the same figure. The entropy contribution from the water should be equal to the difference of total entropy and the entropy loss of the constrained ion pair in the simulations, $T\Delta S_W(r)=T\Delta S(r) - T\Delta S_{IP}$. One of the common features is that the $T\Delta S$, $T\Delta S_W$ and ΔH increase on ion pair approaching and more mildly at the range of 5.0 ~ 12 Å than the region closer than 5.0 Å. The oscillation valleys reflect the characteristic solvation states of the ion pair in the water solution. The neighbor valleys are usually about 2 Å apart. The water solvation structures around the ion pair have been shown in Fig. 6 of ref. 11. The approaching process of ion pair from the infinite distance is intuitively considered as the story that the water molecules escape one after another from the solvation shells of ions with losing the energy of ion-water interaction and gaining the energy of water-water interaction and gaining the entropy of water from the original constrained state to bulk state [9]. The mobility of water increases in this process, when two ions with the opposite charges approach each other. There is a higher barrier between the CIP state and the SSIP state than others, which suggests that the transition between them is controlled by the enthalpy of solution. The relative low enthalpies can be observed at the valleys of the energy curve corresponding to the characteristic states of ion pair, CIP, SIP and 2SIP. Although the qualitative consistency can be reached on the whole, there is a big difference among the selected potentials quantitatively. The main reason behind it is due to the difference of the relative affinities for the ion-water, water-water and ion-ion. The solvation free energy and entropy of single ion Na^+ with the OPLS-SPC/E potential are −88.7 and −0.24 $kcalmol^{-1}$, −74.1 and −48.5 $kcalmol^{-1}$ for Cl^- [42]. The summation of them is lower than the values from other force fields (Table 1), so the changes of enthalpy and entropy during the process of ion pairing, is smaller than those from other potentials. A consistent potential is required to describe a reasonable energy view in the process of ion pairing. Several publications present a decorate work on the optimization of force field parameters based on the LJ potential formed recently, but the consistent accuracy has not yet been achieved [42]. More delicate and flexible potential should be considered to reach this goal, as well as the ion-pair properties, such as scaling factors for the standard combining rules [43].

Conclusions

One of the goals in this work is to explore the ion perturbation on the water H-bond structure and the force field dependent ion clustering, as well as its thermodynamic origin. The BMHTF ion-ion potential and Lennard Jones 12-6 type potential were used to evaluate the effects of the ion-ion potential on the ion clustering and water solvation properties in the NaCl solutions at the concentration of 0.3 $moll^{-1}$, 1 $moll^{-1}$ and 2 $moll^{-1}$. Negligible difference was found for the ion-water and water-water solvation structures with the BMHTF-SPC/E and Dang-SPC/E potentials. An evident difference on the populations of the ion clustering is observed for the different potentials. The existence of ions weakly disturbs the tetrahedral H-bond structure of water beyond the first ion solvation shell. The second and third peaks of the radial distribution functions $g_{OwOw}(r)$ shift inward on adding NaCl into water due to the overlap effect between the contribution from water pairs within the first

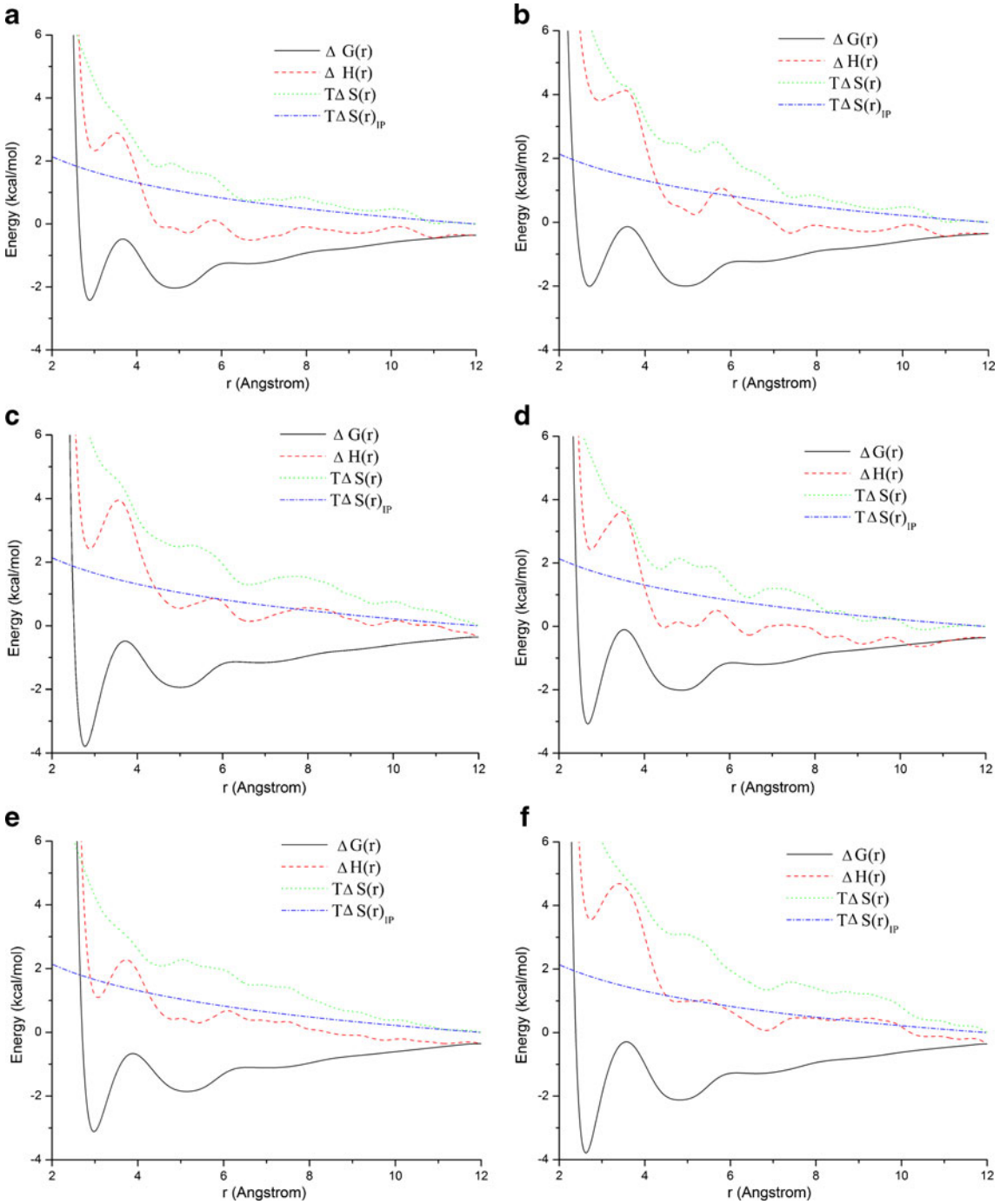

Fig. 7 The relative PMFs, enthalpy, entropy and volume-entropy loss of the constrained ion pair ($W(r)$, $T\Delta S$, ΔH and $T\Delta S_{IP}$) within the distance range of 1.8 ~ 12 Å for the Na^{+}-Cl^{-} ion pair with the Dang-SPC/E (**a**), BMHTF-SPC/E (**b**), AMBER-TIP3P (**c**), CHARMM-TIP3P (**d**), OPLS-TIP3P (**e**) and GROMOS-SPC (**f**) force fields respectively

ion solvation shell and water pairs outside. The reorientation correlation times of water are all in the same level at the different concentrations. A consistent view was shown from both the structural and dynamic angle and a local effect is found for the ions on the water structure and dynamic properties. The anisotropic rotations of water have been observed in the first solvation shells of sodium and chloride.

The association constant of ion pair from the potential of mean force is consistent with the populations of ion clusters in the NaCl solutions at the selected concentration. The aggregation level of ions is sensitive to the potential used in the simulations. The ion-ion interaction potential plays an important role in the forming of the contact ion pair. The thermodynamic quantities were derived from the

temperature dependent PMFs by the constrained molecular dynamics simulations. The entropy of water increases as the ion pair approaches each other and plays an important role in the ion pairing and cluster forming. The kinetic transition of ion pair from the SSIP state to the CIP state is controlled by the enthalpy. Although the overall consistency can be reached qualitatively for the selected force fields, there is a big difference quantitatively. Consistent force fields are needed to reasonably describe the ion clustering and the related properties in electrolyte solutions in the future.

Acknowledgments The authors greatly thank Professor Jay William Ponder for providing the Tinker program. This work is supported by National Natural Science Foundation of China (No. 20873055, 21176029).

References

1. Marcus Y, Hefter G (2006) Ion pairing. Chem Rev 106:4585–4621
2. Fuoss RM (1980) PNAS 77:34–38
3. Omta AW, Kropman MF, Woutersen S, Bakker HJ (2003) Science 301:347–349
4. Skinner JL (2010) Science 328:985–986
5. Tielrooij KJ, Garcia-Araez N, Bonn M, Bakker HJ (2010) Science 328:1006–1009
6. Chandra A (2000) Phys Rev Lett 85:768–771
7. Carrillo-Tripp M, Saint-Martin H, Ortega-Blake I (2003) J Chem Phys 118:7062–7073
8. Mancinelli R, Botti A, Bruni F, Ricci MA, Soper AK (2007) Phys Chem Chem Phys 9:2959–2967
9. Collins KD, Neilson GW, Enderby JE (2007) Biophys Chem 128:95–104
10. Smith DE, Dang LX (1994) J Chem Phys 100:3757–3766
11. Degrève L, da Silva FLB (1999) J Chem Phys 111:5150–5156
12. Chen AA, Pappu RV (2007) J Phys Chem B 111:6469–6478
13. Gu B, Zhang FS, Wang ZP, Zhou HY (2008) J Chem Phys 129:184505–184507
14. Fennell CJ, Bizjak A, Vlachy V, Dill KA (2009) J Phys Chem B 113:6782–6791
15. Timko J, Bucher D, Kuyucak S (2010) J Chem Phys 132: 114510
16. Auffinger P, Cheatham TE III, Vaiana AC (2007) J Chem Theory Comput 3:1851–1859
17. Adams DJ, McDonald IR (1974) J Phys C 7:2761–2775
18. Huggins ML, Mayer JE (1933) J Chem Phys 1:643–646
19. Tosi M, Fumi F (1964) J Phys Chem Solids 25:45–52
20. Åqvist J (1990) J Phys Chem 94:8021–8024
21. Beglov D, Roux B (1994) J Chem Phys 100:9050–9063
22. Jensen KP, Jorgensen WL (2006) J Chem Theor Comput 2:1499–1509
23. Straatsma TP, Berendsen HJC (1988) J Chem Phys 89:5876–5886
24. Berendsen HJC, Grigera JR, Straatsma TP (1987) J Phys Chem 91:6269–6271
25. Jorgensen WL, Chandrasekhar J, Madura JD, Impey RW, Klein ML (1983) J Chem Phys 79:926–935
26. Berendsen HJC, Postma JPM, van Gunsteren WF, Hermans J (1981) In: Pullman B (ed) Intermolecular forces. Reidel, Dordrecht, p 331
27. Sanza E, Vega C (2007) J Chem Phys 126:014507
28. Anwar J, Frenkel D, Noro MG (2003) J Chem Phys 118:728–735
29. Berendsen HJC, Postma JPM, van Gunsteren WF, Di Nola A, Hauk JR (1984) J Chem Phys 81:3684–3690
30. Essmann U, Perera L, Berkowitz ML, Darden T, Lee H, Pedersen LG (1995) J Chem Phys 103:8577–8593
31. Ponder JW, Richards FM (1987) J Comput Chem 8:1016–1024
32. Hess B, Holm C, van der Vegt N (2006) J Chem Phys 124:164509
33. Li J, Car R, Tang C, Wingreen NS (2007) PNAS 104:2626–2630
34. Varma S, Rempe SB (2006) Biophys Chem 124:192–199
35. Chowdhuri S, Chandra A (2003) J Chem Phys 118:9719–9725
36. Laage D, Hynes JT (2006) Science 311:832–835
37. Mancinelli R, Botti A, Bruni F, Ricci MA, Soper AK (2007) J Phys Chem B 111:13570–13577
38. Yang L, Fan Y, Gao YQ (2011) J Phys Chem B 115:12456–12465
39. Mark P, Nilsson L (2001) J Phys Chem A 105:9954–9960
40. Chialvo AA, Simonson JM (2003) J Chem Phys 118:7921–7929
41. Hassan SA (2008) J Phys Chem B 112:10573–10584
42. Horinek D, Mamatkulov SI, Netz RR (2009) J Chem Phys 130:124507–124521
43. Fyta M, Netz RR (2012) J Chem Phys 136:124103